Temporal progression of photosynthetic-strategy in phytoplankton in the Ross Sea, Antarctica

Thomas J. Ryan-Keogh[a1], Liza M. DeLizo[b], Walker O. Smith Jr.[b], Peter N. Sedwick[c], Dennis J. McGillicuddy Jr.[d], C. Mark Moore[a] and Thomas S. Bibby[a]

[a]Ocean and Earth Science, University of Southampton, National Oceanography Centre, Southampton, European Way, Southampton, SO14 3ZH, U.K.
Email: c.moore@noc.soton.ac.uk
Email: tsb@noc.soton.ac.uk
[b]Virginia Institute of Marine Sciences, The College of William and Mary, Gloucester Point, Virginia, 23062, U.S.
Email: delizo@vims.edu
Email: wos@vims.edu
[c]Department of Ocean, Earth and Atmospheric Sciences, Old Dominion University, Norfolk, Virginia, 23529, U.S.
Email: psedwick@odu.edu
[d]Applied Ocean Physics and Engineering, Woods Hole Oceanographic Institute, Woods Hole, Massachusetts, 02543, U.S.
Email: mcgillic@whoi.edu

Author for correspondence email: Thomas.Ryan-Keogh@uct.ac.za

[1] Present address: Southern Ocean Carbon and Climate Observatory, CSIR - Natural Resources and the Environment, 15 Lower Hope Road, Rosebank, Cape Town, 7700, South Africa

Abstract

The bioavailability of iron influences the distribution, biomass and productivity of phytoplankton in the Ross Sea, one of the most productive regions in the Southern Ocean. We mapped the spatial and temporal extent and severity of iron-limitation of the native phytoplankton assemblage using long- (>24 h) and short-term (24 h) iron-addition experiments along with physiological and molecular characterisations during a cruise to the Ross Sea in December-February 2012. Phytoplankton increased their photosynthetic efficiency in response to iron addition, suggesting proximal iron limitation throughout most of the Ross Sea during summer. Molecular and physiological data further indicate that as nitrate is removed from the surface ocean the phytoplankton community transitions to one displaying an iron-efficient photosynthetic strategy characterised by an increase in the size of photosystem II (PSII) photochemical cross section (σ_{PSII}) and a decrease in the chlorophyll-normalised PSII abundance. These results suggest that phytoplankton with the ability to reduce their photosynthetic iron requirements are selected as the growing season progresses, which may drive the well-documented progression from *Phaeocystis antarctica*- assemblages to diatom-dominated phytoplankton. Such a shift in the assemblage-level photosynthetic strategy potentially mediates further drawdown of nitrate following the development of iron deficient conditions in the Ross Sea.

Keywords

Iron, Phytoplankton, Photosynthetic proteins, Photosystem II, Nutrient limitation, Ross Sea

Highlights

- Phytoplankton in the Ross Sea change their photosynthetic physiology over the growing season to a strategy requiring less iron.
- This results in fluorescence yields per chlorophyll and PSII both increasing as the growing season develops.
- This observation may help explain the well characterised seasonal progression from to *Phaeocystis* spp. to diatom spp. over the growing season and also have implications for the assessment of primary production from estimates of chlorophyll in this region.

1. Introduction

The Ross Sea continental shelf is the most productive region in the Southern Ocean (Arrigo and van Dijken, 2004; Peloquin and Smith, 2007), with an annual productivity >200 g C m^{-2} (Smith et al., 2006), which may account for as much as 27% of the estimated total Southern Ocean biological CO_2 uptake (Arrigo et al., 2008). An understanding of the controls on primary productivity is therefore needed given the potential for future changes in stratification (Boyd et al., 2008; Smith et al., 2014) and nutrient inputs to this region (Mahowald and Luo, 2003; Tagliabue et al., 2008).

A persistent polynya in the southern Ross Sea greatly increases in size in the early austral spring (Arrigo and van Dijken, 2003; Reddy et al., 2007), and hosts large seasonal phytoplankton blooms, typically dominated by the colonial haptophyte *Phaeocystis antarctica* (*P. antarctica*) in spring through early summer (November – December), with an increase in abundance of diatoms in mid- to late summer (Arrigo and van Dijken, 2004; Arrigo et al., 1998; DiTullio and Smith, 1996; Goffart et al., 2000; Smith and Gordon, 1997; Smith et al., 2000). Understanding the causes and consequences of this seasonal phytoplankton progression is important, as the spatial and temporal distribution and abundance of *P. antarctica* and diatoms have significant biogeochemical consequences on, for example, the elemental composition and flux of biogenic material from the euphotic zone (Arrigo et al., 1999; DeMaster et al., 1992; Smith and Dunbar, 1998; Tagliabue and Arrigo, 2005).

Iron (Fe) and irradiance are assumed to exert the major 'bottom-up' controls on phytoplankton biogeography and productivity in the Ross Sea, given the incomplete macronutrient removal at the end of the growing season (Arrigo and van Dijken, 2003; Arrigo et al., 1998; Coale et al., 2003; Fitzwater et al., 2000; Sedwick et al., 2000; Sedwick et al., 2007; Smith et al., 2003; Smith et al., 2000; Tagliabue and Arrigo, 2003). Light availability may limit spring phytoplankton growth when vertical mixing is deep and daily integrated irradiance is low, this mixing will also supply dissolved iron (DFe) to the euphotic zone (McGillicuddy et al., 2015). As the growing season progresses and the water column stratifies, the flux of DFe from below is likely reduced and may therefore become a more significant factor in limiting phytoplankton growth rates. Indeed, shipboard iron-addition experiments have repeatedly demonstrated the

role of iron limitation in the Ross Sea (Bertrand et al., 2007; Coale et al., 2003; Cochlan et al., 2002; Martin et al., 1990; Olson et al., 2000; Sedwick and DiTullio, 1997; Sedwick et al., 2000), consistent with other metrics of Fe stress including high levels of flavodoxin (Maucher and DiTullio, 2003) and enhanced biological drawdown of silicate relative to nitrate (Arrigo et al., 2000; Smith et al., 2006).

Changes in phytoplankton composition from *P. antarctica* to diatom species may be linked to the co-limitation and interaction between iron and light. Boyd (2002) speculated that *P. antarctica* growth is limited by Fe availability from spring through late summer. Sedwick et al. (2007) further proposed that decreases in iron availability through spring are mitigated by increases in irradiance, thereby decreasing phytoplankton iron requirements. The differences in intracellular iron requirements alongside changes in the light environment may explain the community succession of the Ross Sea, where diatoms can outcompete *P. antarctica* in the late summer (Strzepek et al., 2012).

Phytoplankton that dominate in the Ross Sea may therefore need to be adapted to highly variable iron concentrations and light availability (Sedwick et al., 2011). An antagonistic relationship between irradiance and photosynthetic Fe demand may be predicted given that lower irradiances can increase Fe requirements associated with the synthesis of the additional photosynthetic units required to increase light absorption (Maldonado et al., 1999; Raven, 1990; Sunda and Huntsman, 1997). Each photosynthetic electron transfer chain requires 22-23 Fe atoms, and the photosynthetic apparatus can be the largest sink of Fe within a phytoplankton cell (Raven, 1990; Shi et al., 2007; Strzepek and Harrison, 2004). In contrast to the tight link between cellular Fe requirements and light harvesting capacity, studies on Southern Ocean diatoms and *P. antarctica* in culture suggest the Fe burden of photosynthesis may be significantly reduced for these species through increases in the size rather than the number of photosynthetic units (termed sigma-type acclimation) in response to iron/ and light limitation (Strzepek et al., 2012; Strzepek et al., 2011). Effectively, these Southern Ocean taxa appear to invest relatively more resources in the generation of a larger light-harvesting apparatus, rather than in the Fe-rich photosynthetic catalysts of photosystems I and II (Strzepek et al., 2012). This Fe-efficient strategy appears to be most pronounced for Southern Ocean diatoms, which, in culture can have some of the largest light harvesting antennae reported (Strzepek et al., 2012), a phenotype which is more commonly associated with small cells (Suggett et al., 2009). The photosynthetic

strategy of Southern Ocean diatoms may therefore contribute to the apparently low Fe requirement and cellular Fe:C ratio of these species (Coale et al., 2003; Kustka et al., 2015; Sedwick et al., 2007; Strzepek et al., 2012; Strzepek et al., 2011), and as such drive the seasonal progression from *P. antarctica* to diatoms in the Ross Sea.

In December-February 2012 a research cruise was conducted as part of the multidisciplinary research project *Processes Regulating Iron Supply at the Mesoscale – Ross Sea* (PRISM-RS), in an effort to identify and quantify the major sources of iron to the surface waters of the Ross Sea during the growing season. As part of this study, physiological and molecular measurements were combined with shipboard incubation experiments in an effort to define the spatial and temporal extent of phytoplankton iron limitation and reveal the photosynthetic strategy of the phytoplankton assemblages.

2. Materials and Methods

2.1. Oceanographic Sampling

The samples and data presented here were obtained during a cruise of the *RVIB Nathaniel B. Palmer* to the Ross Sea (cruise NBP12-01) from 24th December 2011 to 10th February 2012 (DOY 358 – 041). During the cruise, 29 short-term (24 h) and 3 long-term (168 h) incubation experiments were performed (Fig. 1a). Short-term experiments were used to determine rapid iron induced changes in the phytoplankton photophysiological status; whereas long-term experiments determined whether relief from iron limitation could drive changes in biomass. For the long-term incubation experiments, uncontaminated whole seawater was collected from ~5 m depth whilst slowly underway, using a trace-metal clean towed fish system (Sedwick et al., 2011). Uncontaminated whole seawater for the short-term incubation experiments was collected from ~10 m depth in Teflon-lined, external closure 5 L Niskin-X samplers (General Oceanics) deployed on a trace metal clean CTD rosette system (Marsay et al., 2014). Samples for additional analysis were also collected along the cruise track.

2.2. Bioassay Incubation Experiments

Incubation experiments were performed using methods similar to those employed previously in the Southern Ocean (Moore et al., 2007; Nielsdóttir et al., 2012) and the high latitude North Atlantic (HLNA) (Nielsdóttir et al., 2009; Ryan-Keogh et al., 2013). Water for the experiments (see 2.1, above) was transferred unscreened into acid-washed 1.0-L polycarbonate bottles (Nalgene) for the short-term incubation experiments and 4.5-L polycarbonate bottles for the long-term incubation experiments. Incubation bottles were filled in a random order, with triplicate samples for initial measurements in the long-term incubation experiments collected at the beginning, middle and end of the filling process. Initial samples for the short-term incubation experiments were collected from the same Niskin-X sampling bottle. The short-term experiments were run for 24 h and the long-term experiments were run for 168 h; both experiments consisted of two treatments: an unamended control treatment and 2.0 nmol L^{-1} Fe

treatment (hereafter, + Fe). All experimental incubations were conducted as biological duplicates or triplicates.

All bottle tops were externally sealed with film (Parafilm™), and bottles were double bagged with clear polyethylene bags to minimize risks of contamination during the incubation. On-deck incubators were shaded using LEE "blue lagoon" filters to provide light levels corresponding to ~35% of above-surface irradiance (Hinz et al., 2012; Nielsdóttir et al., 2009; Ryan-Keogh et al., 2013). Flowing surface seawater was used to control the temperature in the incubators. Subsampling of long-term incubations for measurements of chlorophyll *a*, dissolved macronutrient concentrations and phytoplankton physiological parameters occurred after 24, 72, 120 and 168 h. Sub-sampling of short-term incubation experiments for the same parameters occurred after 24 h. All experiments were set up and sub-sampled under a class-100 laminar flow hood within a trace metal clean environment.

2.3. Chlorophyll *a* and Nutrient Analysis

Samples for chlorophyll *a* (Chl) analysis (250 mL) were filtered onto GF/F filters and then extracted into 90% acetone for 24 h in the dark at 4°C, followed by analysis with a fluorometer (TD70; Turner Designs) (Welschmeyer, 1994). Macronutrient samples were drawn into 50 mL diluvials and refrigerated at 4°C until analysis, which typically commenced within 12 h of sampling. Nitrate plus nitrite (DIN), phosphate, ammonium and silicate were determined shipboard on a five-channel Lachat Instruments QuikChem FIA+ 8000s series AutoAnalyser (Armstrong et al., 1967; Atlas et al., 1971; Bernhardt and Wilhelms, 1967; Patton, 1983). Dissolved iron was determined post-cruise using flow injection analysis modified from Measures et al. (1995), as described by Sedwick et al. (2011); accuracy of the DFe method was verified by analysis of SAFe reference seawater samples (Johnson et al., 2007).

2.4. Phytoplankton Photosynthetic Physiology

Variable chlorophyll fluorescence was measured using a Chelsea Scientific Instruments Fastracka™ Mk II Fast Repetition Rate fluorometer (FRRf) integrated with a FastAct™ Laboratory system. All samples were acclimated in opaque bottles for 30 minutes at *in situ* temperatures, and FRRf measurements were blank corrected effect using carefully

prepared 0.2 μm filtrates for all samples (Cullen and Davis, 2003). Blanks were typically around 1% and always <10% of the maximum fluorescence signal. Protocols for FRRf measurements and data processing were similar to those detailed elsewhere (Moore et al., 2007). Data from the FRRf were analysed to derive values of the minimum and maximum fluorescence (F_o and F_m) and hence F_v/F_m (where $F_v = F_m - F_o$), as well as the functional absorption cross-section of PSII (σ_{PSII}) by fitting transients to the model of Kolber et al. (1998).

2.5. Phytoplankton Composition

Samples for photosynthetic pigment analysis were collected and measured by high performance liquid chromatography (HPLC). 0.3 – 1.0 L of sea-water were filtered through GF/F filters, which were immediately flash frozen in liquid nitrogen and stored at -80°C until analysis. Pigments were extracted into 90% acetone by sonification before quantification using a Waters Spherisorb ODSU C-18 HPLC column and Waters HPLC system as described in Smith et al. (2006). Algal community composition was then estimated from pigment concentrations following the method of Arrigo et al. (1999).

2.6. Total Protein Extraction and Quantification

Photosynthetic protein abundances were quantified using techniques similar to those described elsewhere (Brown et al., 2008; Macey et al., 2014; Ryan-Keogh et al., 2012). Samples for protein extraction were collected by filtering 1.0-3.0 L of seawater onto GF/F filters (Whatman) under low light for ~45 minutes to minimize changes in protein abundance following sampling. Filters were flash frozen and stored at -80°C until analysis. Proteins were extracted in the laboratory according to the protocol described by Brown et al. (2008). Quantification was performed using custom Agrisera™ primary antibodies and peptide standards, which were designed against peptide tags conserved across all oxygenic photosynthetic species for protein subunits that are representative of the functional photosynthetic complex PsbA (PSII) (Campbell et al., 2003). Protein abundances were quantified using QuantityOne™ and ImageLab™ software; quantification was performed within the unsaturated portion of the calibration curve. The estimated protein abundances were comparable to those reported for natural

239 phytoplankton communities using similar methods (Hopkinson et al., 2010; Losh et al.,
240 2013; Macey et al., 2014; Richier et al., 2012).
241

3. Results and Discussion

3.1. General Oceanography

A range of oceanographically distinct regions was occupied on the Ross Sea continental shelf during the PRISM-RS cruise (Fig. 1). These included areas close to the Ross Ice Shelf, near and within pack ice, and over shallow bathymetric features, both of which may provide important sources of DFe to the upper water column (McGillicuddy et al., 2015). Highest chlorophyll a concentrations (Fig. 2a) were associated with the ice-shelf in the southwestern Ross Sea (24.6 μg Chl L^{-1}) and correlated with the lowest DIN (dissolved inorganic nitrate + nitrite) concentrations (Figs. 2b, 3) and lowest surface F_v/F_m values observed (Figs. 2c, 3). Surface DFe concentrations ranged from 0.067-0.787 nM (Fig. 2d), were not correlated with chlorophyll or DIN concentrations (Fig. 3, Supplementary Information, Fig. S1), and were elevated off the continental shelf in the northeast sector of the Ross Sea.

3.2. Mapping of Iron Limitation

Despite being the most productive region in the Southern Ocean, our results confirm that phytoplankton growth in the Ross Sea is limited by iron availability during summer, consistent with previous studies (Bertrand et al., 2011; Bertrand et al., 2007; Coale et al., 2003; Cochlan et al., 2002; Martin et al., 1990; Olson et al., 2000; Sedwick and DiTullio, 1997; Sedwick et al., 2000). The response of phytoplankton to iron-addition was assayed through a series of long- (168 h) and short-term (24 h) iron-addition incubations (Fig. 1), while no clear spatial pattern in iron stress could be observed from a single cruise during a time of relatively rapid changes in a spatio-temporally complex system (Fig. 2), there was evidence of an increase in photosynthetic efficiency following iron addition throughout much of the Ross Sea during summer, highlighting the role of iron in influencing phytoplankton physiology. To compare these iron-mediated changes in F_v/F_m, $\Delta(F_v/F_m)$ was calculated as defined in Ryan-Keogh et al. (2013), as the difference between the Fe-amended and control treatments (Equation 1).

Equation 1 Calculation of $\Delta(F_v/F_m)$.

$$\Delta\,(F_v/F_m) = \frac{F_v/F_{m_{+Fe}} - F_v/F_{m_{Control}}}{Time}$$

Values of $\Delta(F_v/F_m)$ were frequently positive following iron addition (ranging from 0.00 - 0.17) (Fig. 4a), suggesting that Fe amendments increased the photosynthetic efficiency of phytoplankton in much of the Ross Sea during the sampling period.

Data from long-term (168 h) experiments (Table 1 and Fig. 4) enable a more detailed analysis of the response of phytoplankton to iron-additions. Three experiments were initiated from (1) near the Ross Ice Shelf, (2) over the Ross Bank and (3) in an anti-cyclonic eddy (Figs. 1 and 4). The three experiments revealed varying responses to iron additions by the extant phytoplankton assemblage. Experiments 1 and 3 gave a strong and positive response to iron additions, and provided evidence that phytoplankton were iron limited. Shorter-term responses revealed elevated values of F_v/F_m (i.e., a positive $\Delta(F_v/F_m)$) after 24 h (Fig. 4a), with subsequent significant (ANOVA, $p<0.05$) increases in growth rates and nutrient removal observed after 168 h (Table 1). Experiment 2, initiated over the Ross Bank, did not show an increase in photosynthetic efficiency $\Delta(F_v/F_m)$ (Fig. 4a). Moreover, growth rate and nutrient removal were not significantly different between control and iron-addition conditions until after >168 h (ANOVA, $p>0.05$) (Table 1), which most likely reflects severe depletion of ambient DFe in the control treatments by this time. The Ross Bank (Fig. 4a, Table 1) has a shallow bathymetry (~150 m), and none of the Fe-addition experiments in this region showed a significant response (Fig. 4). The Ross Bank may therefore provide significant and continuous DFe inputs to the euphotic zone, thereby ultimately stimulating productivity.

The measurement of F_v/F_m is derived from analysis of the fluorescence kinetics emitted from the photosynthetic reaction centre photosystem II (PSII) and its associated light-harvesting antenna (Kolber and Falkowski, 1993). Understanding the mechanism of changes to F_v/F_m can provide information on the process by which phytoplankton respond to iron-limitation. Absolute changes in maximum fluorescence (F_m) and variable fluorescence (F_v) normalised to chlorophyll *a* were calculated (Figs. 4b and c), revealing a significant difference between the +Fe and control treatments in F_m Chl^{-1} (t = 24 h (*t*-test, $p<0.05$)), whereas there was no significant difference for F_v Chl^{-1} (t = 24 h (*t*-test, $p>0.05$)). This suggests that changes in F_v/F_m reflect changes in the proportion of chlorophyll that is photosynthetically coupled to active PSII reaction centres, rather

than changes in the activity of PSII (Behrenfeld et al., 2006; Lin et al., 2016; Macey et al., 2014). A similar response was observed for all short-term iron-addition experiments that exhibited positive changes in $\Delta(F_v/F_m)$.

3.3 Temporal Development of Photosynthetic Strategy

Given the high degree of spatial variability in response to iron-additions, we placed all observations within a unified framework, hence producing a conceptualised model of temporal progression of phytoplankton within the Ross Sea. The PRISM-RS cruise sampled for 30 days covering a period from mid- to late summer, during which we expected iron limitation of phytoplankton growth to be significant (Sedwick et al., 2000). Total phytoplankton biomass accumulation is dependent on growth after the sampled regions become ice-free (Arrigo and van Dijken, 2003) and the losses due to grazing, sinking and physical removal. All spatial data therefore represent a mosaic of different temporal progressions that represent different stages of phytoplankton development. We utilise surface nitrate (DIN) as a proxy to separate the temporal patterns from any spatial differences (Fig. 5). As phytoplankton biomass (Chl) increased, nutrients were removed and F_v/F_m reduced (Figs. 3, 5a). Pigment data showed that the nutrient drawdown and Chl increase in parallel with a shift from *P. antarctica*-dominated to diatom-dominated assemblages (Figs. 3, 5b). Within this conceptual framework, the relative severity of Fe-stress ($\Delta F_v/F_m$) may be inferred from the Fe-addition incubation experiments. Two potential phases of Fe deficiency were identified (Fig. 5c): first, when DIN concentrations remain high (> ~20 μM) and *P. antarctica* is a major component of the phytoplankton (labelled '1'), and secondly when DIN is further removed (to < ~20 μM) by diatom-dominated communities (labelled '2'; Fig. 5c).

Photophysiological parameters are presented within this framework. The relative size of the effective light-harvesting cross-section of PSII (σ_{PSII}) (Fig. 6a) is low (~1.6 nm^{-2}) when DIN and F_v/F_m are high, and approximately doubles to ~3.29 nm^{-2} as DIN is depleted and the assemblage becomes diatom-dominated. Quantification of the photosynthetic catalyst PSII further characterises the photosynthetic strategy of phytoplankton in the Ross Sea. Chlorophyll normalised to abundances of the protein target PsbA (indicative of the abundance of PSII; (Brown et al., 2008) (Chl:PsbA), which can provide another indication of the relative sizes of the light harvesting

pigment antenna relative the abundance of the photosystems, is lower at higher DIN concentrations and increases as DIN and F_v/F_m decrease (Fig. 6b). Combining the protein abundance data and the photophysiological measurements, the maximum fluorescent yield per chlorophyll (F_m:Chl) (Fig. 6c) and per PSII (F_m:PsbA) (Fig. 6d) can also be calculated. Both of these parameters increase, by 46 and 296% respectively, with decreases in DIN and F_v/F_m.

Together, these photophysiological measurements and corresponding environmental information at the time of sampling therefore indicate several significant correlations (Fig. 3 & Supplementary Information, S1) associated with the potential drivers of the observed transition in community structure and subsequent changes in photophysiology. Thus, within our conceptual frame work, using DIN concentration as a proxy for the stage of the phytoplankton bloom, we observe statistically significant positive correlations ($p<0.01$) with other macronutrients and the photosynthetic efficiency (F_v/F_m) which all decline as nitrate is removed from the system. While negative correlations ($p<0.01$) are observed between DIN and temperature, chlorophyll concentration, the relative abundance of diatoms and σ_{PSII} which all increase as nitrate is removed from the system. While no significant correlation is seem between DIN and the fluorescence yield per PSII (F_m:PSII) or the chlorophyll content per PSII (Chl:PSII), there is a significant negative correlation between F_m:Chl and PSII:Chl ($p<0.01$) (Fig. 3).

No statistically significant ($p<0.01$) relationships were observed with dissolved iron concentrations, suggesting that this variable may not represent a good indicator of iron stress, as might be expected considering that any limiting nutrient would be expected to be severely depleted by biological uptake. Overall, the observed correlations are thus taken to be indicative of the phytoplankton community transitioning between dominant groups as SST increases, non-limiting macronutrients are drawn down and the community biomass increases, potential as a result of different Fe utilisation capacities between diatoms and *P. antarctica* (Strzepek et al., 2012). These observations may also support that the hypothesis that Southern Ocean diatoms may both acquire (Kustka et al., 2015) and utilise (Strzepek et al., 2012) iron more effectively than *P. antarctica* and that the community transition may enable further drawdown of nitrate.

While there can be an array of reasons for diatoms being better at acquiring and utilising available DFe as it becomes limiting during summer in the Ross Sea, differences in photosynthetic strategy have the potential to be a significant factor in

regulating the temporal changes that occur, given that the photosynthetic apparatus represents the dominant sink for Fe in a phytoplankton cell (Raven, 1990; Strzepek and Harrison, 2004). The analysis presented here clearly demonstrates that a different photosynthetic strategy is apparent within the phytoplankton community responsible for the initial DIN removal vs. those responsible for the later DIN removal. These observations of photosynthetic strategy are consistent with some of the ecophysiological differences observed within culture-based studies of Southern Ocean phytoplankton (Strzepek et al., 2012). Phytoplankton in the Ross Sea generally display a large, functional light-harvesting cross section for PSII (σ_{PSII}) compared to temperate species (Smith et al., 2011). As has been proposed (Strzepek et al., 2012), this may reflect a strategy by which cells acclimate and/or adapt through increasing the size of photosynthetic units rather than the number of photosynthetic units in a low Fe environment – thus escaping the typical antagonistic relationship between iron-demand and light capture (Sunda and Huntsman, 1997). Our measurements of the abundance of the photosynthetic catalysis PSII were also consistent with such an observation, whereby the increase in the ratio of Chl:PSII mirrors the increase in σ_{PSII}. (Fig. 6b). This strategy could significantly reduce the iron-demand normally associated with the photosynthetic apparatus. Phytoplankton that dominate at low DIN have a particularly large σ_{PSII} and have increased Chl:PSII values by 255%, again in agreement with culture studies in which Southern Ocean diatoms have larger σ_{PSII} than *P. antarctica* (Strzepek et al., 2012).

We thus suggest that the diatoms that dominate in summer as DIN is removed may represent a refined strategy to reduced iron availability, noting that previous information from temperate taxa and regions (Suggett et al., 2009) would tend to suggest that relatively high functional cross sections would be unlikely in phytoplankton with large cell sizes typical of many Southern Ocean diatoms (Suggett et al., 2009). Large cells with large σ_{PSII} may, however, result in ecophysiological trade-offs, including a tendency for over-excitation of PSII and photodamage, which may require a rapid PSII repair cycle or a requirement for rapidly inducible and significant non-photochemical quenching (Campbell and Tyystjärvi, 2012; Petrou et al., 2010; Wu et al., 2011), possibly suggesting Antarctic diatoms would require novel photoprotective strategies. Despite these potential negative consequences of a large σ_{PSII}, Antarctic diatoms seem to have adopted a phenotypic response underlining the

409 relevance of iron-availability and providing some explanation for the low Fe:C ratios
410 in some of these species (Strzepek et al., 2012).

411 While the observations in this study were restricted to the summer season they
412 do include DIN concentrations similar to those estimated for the winter mixed layer
413 nitrate concentration (McGillicuddy et al., 2015) and so potentially conditions
414 analogous to a broader seasonal progression in phytoplankton composition in the Ross
415 Sea from *P. antarctica* early in the growing season to diatom-dominance later in
416 summer (Smith et al., 2010). The dataset therefore provides indications of potential
417 contributory mechanisms for this seasonal progression, while also reflecting the large
418 degree of spatial heterogeneity in physical and biological processes throughout the
419 growing season in the Ross Sea (Smith and Jones, 2015).

420 The data presented here also provide insights into the mechanism of the iron-
421 stress response of phytoplankton. Increases in F_v/F_m are commonly reported as a
422 response to Fe addition (Boyd et al., 2008; Feng et al., 2010). Results from the
423 experiments and observations show that increases in F_v/F_m in response to Fe addition
424 and elevated F_v/F_m values in regions with modest DIN drawdown result from reduction
425 in the ratio of F_m:Chl (or F_m:PSII) rather than changes in F_v:Chl. This is in agreement
426 with similar observations from the high latitude North Atlantic and Equatorial Pacific
427 (Behrenfeld et al., 2006; Lin et al., 2016; Macey et al., 2014) regions and implies that
428 low F_v/F_m results from changes in the coupling of light-harvesting chlorophyll-binding
429 proteins to photosynthesis rather than accumulation of damaged photosystems. Such
430 accumulation of non-photosynthetically active chlorophyll-binding proteins in Fe-
431 limited oceanic regions can have consequences on estimates of productivity in these
432 regions (Behrenfeld et al., 2006).

4. Conclusions

The current study represents an analysis of the summer photosynthetic strategies of phytoplankton in the Ross Sea and highlights how different iron-efficiency strategies occur in phytoplankton as Fe becomes limiting and irradiance availability becomes maximal. This is important for understanding Fe usage efficiency in the region. The Ross Sea clearly differs from other high latitude regions due to plankton composition, yet iron availability still contributes to reduced growth rates and macronutrient removal. Even though this system is one of the most productive regions in the Southern Ocean, iron availability still exerts a strong control over summer productivity and biomass accumulation, and any changes in future iron supply induced by climate change could have profound effects. Climate-mediated changes to the mixed layer depth and sea-ice cover could change iron limitation strategies and phytoplankton phenology (Boyd et al., 2012), as well as alterations to iron supply from highly variable supply mechanisms such as Australian and local dust inputs (Mackie et al., 2008). The Southern Ocean is predicted to be particularly biogeochemically significant with respect to climate change (Marinov et al., 2006) and is the only iron-limited HNLC region where the cryosphere plays a major role. An understanding of the role of iron limitation in this highly dynamic environment is thus particularly important; particularly as climate mediated variability is expected to increase.

Acknowledgements

We thank the captain and crew of the RVIB *Nathaniel B. Palmer* during research cruise NBP12-01, alongside all the scientists involved in the cruise. Chris Marsay performed the DFe determinations. This research was supported by grants from the National Science Foundation (ANT-0944254 to W.O.S., ANT-0944174 to P.N.S.), and a NERC PhD studentship to TRK.

5. References

Armstrong, F.A.J., Stearns, C.R., Strickland, J.D.H., 1967. The measurement of upwelling and subsequent biological processes by means of the Technicon AutoAnalyzer and associate equipment. Deep-Sea Research 14, 381-389.

Arrigo, K.R., DiTullio, G.R., Dunbar, R.B., Robinson, D.H., VanWoert, M., Worthen, D.L., Lizotte, M.P., 2000. Phytoplankton taxonomic variability in nutrient utilization and primary production in the Ross Sea. J Geophys Res 105, 8827-8845.

Arrigo, K.R., Robinson, D.H., Worthen, D.L., Dunbar, R.B., DiTullio, G.R., VanWoert, M., Lizotte, M.P., 1999. Phytoplankton community structure and the drawdown of nutrients and CO_2 in the Southern Ocean. Science 283, 365-367.

Arrigo, K.R., van Dijken, G.L., 2003. Phytoplankton dynamics within 37 Antarctic coastal polynya systems. J Geophys Res 108, 3271.

Arrigo, K.R., van Dijken, G.L., 2004. Annual changes in sea-ice, chlorophyll a, and primary production in the Ross Sea, Antarctica. Deep-Sea Research II 51, 117-138.

Arrigo, K.R., van Dijken, G.L., Long, M., 2008. Coastal Southern Ocean: A strong anthropogenic CO_2 sink. Geophysical Research Letters 35, L21602.

Arrigo, K.R., Worthen, D., Schnell, A., Lizotte, M.P., 1998. Primary production in Southern Ocean waters. J Geophys Res 103, 15587-15600.

Atlas, e.l., Hager, S.W., Gordon, L.I., Park, P.K., 1971. A practical manual for use of the Technicon Autoanalyzer in seawater nutrient analyses: revised, Technical Report 215. Oregon State University, p. 48.

Behrenfeld, M.J., Worthington, K., Sherrell, R.M., Chavez, F.P., Strutton, P., McPhaden, M., Shea, D.M., 2006. Controls on tropical Pacific Ocean productivity revealed through nutrient stress diagnostics. Nature 442, 1025-1028.

Bernhardt, H., Wilhelms, A., 1967. The continuous determination of low level iron, soluble phosphate and total phosphate with the AutoAnalyzer, Technicon Symposium, p. 386.

Bertrand, E.M., Saito, M.A., Lee, P.A., Dunbar, R.B., Sedwick, P.N., Ditullio, G.R., 2011. Iron limitation of a springtime bacterial and phytoplankton community in the Ross Sea: implications for vitamin b(12) nutrition. Frontiers in microbiology 2, 160.

491 Bertrand, E.M., Saito, M.A., Rose, J.M., Riesselman, C.R., Lohan, M.C., Noble, A.E.,
492 Lee Peter, A., DiTullio, G.R., 2007. Vitamin B12 and iron co-limitation of
493 phytoplankton growth in the Ross Sea. Limnol Oceanogr 52, 1078-1093.
494 Boyd, P.W., 2002. Environmental factors controlling phytoplankton processes in the
495 Southern Ocean. J Phycol 38, 844-861.
496 Boyd, P.W., Arrigo, K.R., Strzepek, R., van Dijken, G.L., 2012. Mapping
497 phytoplankton iron utilization: Insights into Southern Ocean supply mechanisms. J
498 Geophys Res 117, C06009.
499 Boyd, P.W., Doney, S.C., Strzepek, R., Dusenberry, J., Lindsay, K., Fung, I., 2008.
500 Climate-mediated changes to mixed-layer properties in the Southern Ocean: assessing
501 the phytoplankton response. Biogeosciences 5, 847-864.
502 Brown, C.M., MacKinnon, J.D., Cockshutt, A.M., Villareal, T.A., Campbell, D.A.,
503 2008. Flux capacities and acclimation costs in *Trichodesmium* from the Gulf of
504 Mexico. Marine Biology 154, 413-422.
505 Campbell, D.A., Cockshutt, A.M., Porankiewicz-Asplund, J., 2003. Analysing
506 photosynthetic complexes in uncharaterized species or mixed microalgal communities
507 using global antibodies. Physiol Plant 119, 322-327.
508 Campbell, D.A., Tyystjärvi, E., 2012. Parameterization of photosystem II
509 photoinactivation and repair. Biochim Biophys Acta 1817, 258-265.
510 Coale, K.H., Wang, X.J., Tanner, S.J., Johnson, K.S., 2003. Phytoplankton growth
511 and biological response to iron and zinc addition in the Ross Sea and Antarctic
512 Circumpolar Current along 170 degrees W. Deep-Sea Research II 50, 635-653.
513 Cochlan, W.P., Bronk, D.A., Coale, K.H., 2002. Trace metals and nitrogenous
514 nutrition of Antarctic phytoplankton: experimental observations in the Ross Sea.
515 Deep-Sea Research II 49, 3365-3390.
516 Cullen, J.J., Davis, R.F., 2003. The blank can make a big difference in oceanographic
517 measurements. Limnology and Oceanography Bulletin 12, 29-35.
518 DeMaster, D.j., Dunbar, R.B., Gordon, L.I., Leventer, A.R., Morrison, J.M., Nelson,
519 D.M., Nittrouer, C.A., Smith, W.O., Jr., 1992. Cycling and accumulation of biogenic
520 silica and organic matter in high-latitude environments: The Ross Sea. Oceanography
521 5, 146-153.
522 DiTullio, G.R., Smith, W.O., 1996. Spatial patterns in phytoplankton biomass and
523 pigment distributions in the Ross Sea. J Geophys Res 101, 18467-18477.

524 Feng, Y., Hare, C.E., Rose, J.M., Handy, S.M., DiTullio, G.R., Lee, P.A., Smith,
525 W.O., Jr., Peloquin, J., Tozzi, S., Sun, J., Zhang, Y., Dunbar, R.B., Long, M.C.,
526 Sohst, B., Lohan, M., Hutchins, D.A., 2010. Interactive effects of iron, irradiance and
527 CO_2 on Ross Sea phytoplankton. Deep-Sea Research I 57, 368-383.
528 Fitzwater, S.E., Johnson, K.S., Gordon, R.M., Coale, K.H., Smith, W.O., Jr., 2000.
529 Trace metal concentrations in the Ross Sea and their relationship with nutrients and
530 phytoplankton growth. Deep-Sea Research II 47, 3159-3179.
531 Goffart, A., Catalano, G., Hecq, J.H., 2000. Factors controlling the distribution of
532 diatoms and *Phaeocystis* in the Ross Sea. Journal of Marine Systems 27, 161-175.
533 Hinz, D.J., Nielsdóttir, M.C., Korb, R.E., Whitehouse, M.J., Poulton, A.J., Moore,
534 C.M., Achterberg, E.P., Bibby, T.S., 2012. Responses of microplankton community
535 structure to iron addition in the Scotia Sea. Deep-Sea Research II 59, 36-46.
536 Hopkinson, B.M., Xu, Y., Shi, D., McGinn, P.J., Morel, F.M.M., 2010. The effect of
537 CO_2 on the photosynthetic physiology of phytoplankton in the Gulf of Alaska. Limnol
538 Oceanogr 55, 2011-2024.
539 Johnson, K.S., Elrod, V.A., Fitzwater, S.E., Plant, J., Boyle, E., Bergquist, B.,
540 Bruland, K.W., Aguilar-Islas, A.M., Buck, K., Lohan, M.C., Smith, G.J., Sohst, B.M.,
541 Coale, K.H., Gordon, M., Tanner, S., Measures, C.I., Moffett, J., Barbeau, K.A.,
542 King, A., Bowie, A.R., Chase, Z., Cullen, J.J., Laan, P., Landing, W., Mendez, J.,
543 Milne, A., Obata, H., Doi, T., Ossiander, L., Sarthou, G., Sedwick, P.N., Van den
544 Berg, S., Laglera-Baquer, L., Wu, J.-F., Cai, Y., 2007. Developing standards for
545 dissolved iron in seawater. Eos, Transactions American Geophysical Union 88, 131-
546 132.
547 Kolber, Z.S., Falkowski, P.G., 1993. Use of active fluorescence to estimate
548 phytoplankton photosynthesis in situ. Limnol Oceanogr 38, 1646-1665.
549 Kolber, Z.S., Prášil, O., Falkowski, P.G., 1998. Measurements of variable chlorophyll
550 fluorescence using fast repetition rate techniques: defining methodology and
551 experimental protocols. Biochim Biophys Acta 1367, 88-106.
552 Kustka, A.B., Jones, B.M., Hatta, M., Field, M.P., Milligan, A.J., 2015. The influence
553 of iron and siderophores on eukaryotic phytoplankton growth rates and community
554 composition in the Ross Sea. Mar Chem 173, 195-207.
555 Lin, H., Kuzimov, F.I., Park, J., Lee, S., Falkowski, P.G., Gorbunov, M.Y., 2016. The
556 fate of photons absorbed by phytoplankton in the global ocean. Science 351, 264-267.

557 Losh, J.L., Young, J.N., Morel, F.M.M., 2013. Rubisco is a small fraction of total
558 protein in marine phytoplankton. New Phytol 198, 52-58.
559 Macey, A.I., Ryan-Keogh, T.J., Richier, S., Moore, C.M., Bibby, T.S., 2014.
560 Photosynthetic protein stoichiometry and photophysiology in the high latitude North
561 Atlantic. Limnol Oceanogr 59, 1853-1864.
562 Mackie, D.S., Boyd, P.W., McTainsh, G.H., Tindale, N.W., Westberry, T.K., Hunter,
563 K.A., 2008. Biogeochemistry of iron in Australian dust: From eolian uplift to marine
564 uptake. Geochemistry, Geophysics, Geosystems 9, Q03Q08.
565 Mahowald, N.M., Luo, C., 2003. A less dusty future? Geophysical Research Letters
566 30, 1903 doi:1910.1029/2003GL917880.
567 Maldonado, M.T., Boyd, P.W., Harrison, P.J., Price, N.M., 1999. Co-limitation of
568 phytoplankton growth by light and Fe during winter in the NE subarctic Pacific
569 Ocean. Deep-Sea Research II 46, 2475-2485.
570 Marinov, I., Gnanadesikan, A., Toggweiler, J.R., Sarmiento, J.L., 2006. The Southern
571 Ocean biogeochemical divide. Nature 441, 964-967.
572 Marsay, C.M., Sedwick, P.N., Dinniman, M.S., Barrett, P.M., Mack, S.L.,
573 McGillicuddy, D.J., 2014. Estimating the benthic efflux of dissolved iron on the Ross
574 Sea continental shelf. Geophysical Research Letters 41, 7576-7583.
575 Martin, J.H., Gordon, R.M., Fitzwater, S.E., 1990. Iron in Antarctic waters. Nature
576 345, 156-158.
577 Maucher, J.M., DiTullio, G.R., 2003. Flavodoxin as a diagnostic indicator of chronic
578 iron limitation in the Ross Sea and New Zealand sector of the Southern Ocean,
579 Biogeochemistry of the Ross Sea. American Geophysical Union, Washington D.C.,
580 pp. 35-52.
581 McGillicuddy, D.J., Sedwick, P.N., Dinniman, M.S., Arrigo, K.R., Bibby, T.S.,
582 Greenan, B.J.W., Hofmann, E.E., Klinck, J.M., Smith, W.O., Jr., Mack, S.L., Marsay,
583 C.M., Sohst, B.M., van Dijken, G.L., 2015. Iron supply and demand in an Antarctic
584 shelf ecosystem. Geophysical Research Letters.
585 Measures, C.I., Yuan, J., Resing, J.A., 1995. Determination of iron in seawater by
586 flow injection analysis using in-line preconcentration and spectrophotometric
587 detection. Mar Chem 50, 3-12.
588 Moore, C.M., Seeyave, S., Hickman, A.E., Allen, J.T., Lucas, M.I., Planquette, H.,
589 Pollard, R.T., Poulton, A.J., 2007. Iron-light interactions during the CROZet natural

590 iron bloom and EXport experiment (CROZEX) I: Phytoplankton growth and
591 photophysiology. Deep-Sea Research II 54, 2045-2065.
592 Nielsdóttir, M.C., Bibby, T.S., Moore, C.M., Hinz, D.J., Sanders, R., Whitehouse, M.,
593 Korb, R., Achterberg, E.P., 2012. Seasonal and spatial dynamics of iron availability in
594 the Scotia Sea. Mar Chem 130, 62-72.
595 Nielsdóttir, M.C., Moore, C.M., Sanders, R., Hinz, D.J., Achterberg, E.P., 2009. Iron
596 limitation of the postbloom phytoplankton communities in the Iceland Basin. Global
597 Biogeochemical Cycles 23, 1-13.
598 Olson, R.J., Sosik, H.M., Chekalyuk, A.M., Shalapyonok, A., 2000. Effects of iron
599 enrichment on phytoplankton in the Southern Ocean during late summer: active
600 fluorescence and flow cytometric analyses. Deep-Sea Research II 47, 3181-3200.
601 Patton, C.J., 1983. Design, characterization and applications of a miniature continous
602 flow analysis system. Michigan State University, Ann Arbor, Michigan.
603 Peloquin, J.A., Smith, W.O., Jr., 2007. Phytoplankton blooms in the Ross Sea,
604 Antarctica: Interannual variability in magnitude, temporal patterns, and composition. J
605 Geophys Res 112, C08013.
606 Petrou, K., Hill, R., Brown, C.M., Campbell, D.A., Doblin, M.A., Ralph, P.J., 2010.
607 Rapid photoprotection in sea-ice diatoms from the East Antarctic pack ice. Limnol
608 Oceanogr 55, 1400-1407.
609 Raven, J.A., 1990. Predictions of Mn and Fe use efficiencies of phototrophic growth
610 as a function of light availability for growth and C assimilation pathway. New Phytol
611 116, 1-18.
612 Reddy, T.E., Arrigo, K.R., Holland, D.M., 2007. The role of thermal and mechanical
613 processes in the formation of the Ross Sea summer polynya. J Geophys Res 112.
614 Richier, S., Macey, A.I., Pratt, N.J., Honey, D.J., Moore, C.M., Bibby, T.S., 2012.
615 Abundances of Iron-Binding Photosynthetic and Nitrogen-Fixing Proteins of
616 Trichodesmium Both in Culture and In Situ from the North Atlantic. Plos One 7,
617 e35571.
618 Ryan-Keogh, T.J., Macey, A.I., Cockshutt, A.M., Moore, C.M., Bibby, T.S., 2012.
619 The cyanobacterial chlorophyll-binding-protein IsiA acts to increase the *in vivo*
620 effective absorption cross-section of photosystem I under iron limitation. J Phycol 48,
621 145-154.
622 Ryan-Keogh, T.J., Macey, A.I., Nielsdóttir, M., Lucas, M.I., Steigenberger, S.S.,
623 Stinchcombe, M.C., Achterberg, E.P., Bibby, T.S., Moore, C.M., 2013. Spatial and

624 temporal development of phytoplankton iron stress in relation to bloom dynamics in
625 the high-latitude North Atlantic Ocean. Limnol Oceanogr 58, 533-545.
626 Sedwick, P.N., DiTullio, G.R., 1997. Regulation of algal blooms in Antarctic shelf
627 waters by the release of iron from melting sea ice. Geophysical Research Letters 24,
628 2515-2518.
629 Sedwick, P.N., DiTullio, G.R., Mackey, D.J., 2000. Iron and manganese in the Ross
630 Sea, Antarctica: seasonal iron limitation in Antarctic shelf waters. J Geophys Res 105,
631 11321-11336.
632 Sedwick, P.N., Garcia, N.S., Riseman, S.F., Marsay, C.M., DiTullio, G.R., 2007.
633 Evidence for high iron requirements of colonial *Phaeocystis antarctica* at low
634 irradiance. Biogeochemistry 83, 83-97.
635 Sedwick, P.N., Marsay, C.M., Sohst, B.M., Aguilar-Islas, A.M., Lohan, M.C., Long,
636 M.C., Arrigo, K.R., Dunbar, R.B., Saito, M.A., Smith, W.O., Jr., DiTullio, G.R.,
637 2011. Early season depletion of dissolved iron in the ross Sea polynya: implications
638 for iron dynamics on the Antarctic continental shelf. J Geophys Res 116, C12019.
639 Shi, T., Sun, Y., Falkowski, P.G., 2007. Effects of iron limitation on the expression of
640 metabolic genes in the marine cyanobacterium *Trichodesmium erythraeum* IMS101.
641 Environmental Microbiology 9, 2945-2956.
642 Smith, W.O.J., Asper, V.A., Tozzi, S., Liu, X., Stammerjohn, S.E., 2011. Surface
643 layer variability in the Ross Sea, Antarctica as assessed by in situ fluorescence
644 measurements. Progress in Oceanography 88, 28-45.
645 Smith, W.O.J., Dennett, M.R., Mathot, S., Caron, D.A., 2003. The temporal dynamics
646 of the flagellated and colonial stages of Phaeocystis antarctica in the Ross Sea. Deep-
647 Sea Research II 50, 605-617.
648 Smith, W.O.J., Dinniman, M.S., Hoffman, E.E., Klinck, J.M., 2014. The effects of
649 changing winds and temperatures on the oceanography of the Ross Sea in the 21st
650 century. Geophysical Research Letters 41, 1624-1631.
651 Smith, W.O.J., Dinniman, M.S., Tozzi, S., DiTullio, G.R., Mangoni, O., Modigh, M.,
652 Saggiomo, V., 2010. Phytoplankton photosynthetic pigments in the Ross Sea: Patterns
653 and relationships among functional groups. Journal of Marine Systems 82, 177-185.
654 Smith, W.O.J., Dunbar, R.B., 1998. The relationship between new production and
655 vertical flux on the Ross Sea continental shelf. Journal of Marine Systems 17, 445-
656 457.

Smith, W.O.J., Gordon, L.I., 1997. Hyperproductivity of the Ross Sea (Antarctica) polynya during austral spring. Geophysical Research Letters 24, 233-236.

Smith, W.O.J., Jones, R.M., 2015. Vertical mixing, critical depths, and phytoplankton growth in the Ross Sea. ICES J Mar Sci 72, 1952-1960.

Smith, W.O.J., Marra, J., Hiscock, M.R., Barber, R.T., 2000. The seasonal cycle of phytoplankton biomass and primary productivity in the Ross Sea, Antarctica. Deep-Sea Research II 47, 3119-3140.

Smith, W.O.J., Shields, A.R., Peloquin, J.A., Catalano, G., Tozzi, S., Dinniman, M.S., Asper, V.A., 2006. Interannual variations in nutrients, net community production, and biogeochemical cycles in the Ross Sea. Deep-Sea Research II 53, 815-833.

Strzepek, R.F., Harrison, P.J., 2004. Photosynthetic architecture differs in coastal and oceanic diatoms. Nature 431, 689-692.

Strzepek, R.F., Hunter, K.A., Frew, R.D., Harrison, P.J., Boyd, P.W., 2012. Iron-light interactions differ in Southern Ocean phytoplankton. Limnol Oceanogr 57, 1182-1200.

Strzepek, R.F., Maldonado, M.T., Hunter, K.A., Frew, R.D., Boyd, P.W., 2011. Adaptive strategies by Southern Ocean phytoplankton to lessen iron limitation: Uptake of organically complexed iron and reduced cellular iron requirements. Limnol Oceanogr 56, 1983-2002.

Suggett, D.J., Moore, C.M., Hickman, A.E., Geider, R.J., 2009. Interpretation of fast repetition rate (FRR) fluorescence: signatures of phytoplankton community structure versus physiological state. Mar Ecol Prog Ser 376, 1-19.

Sunda, W.G., Huntsman, S.A., 1997. Interrelated influence of iron, light and cell size on marine phytoplankton growth. Nature 390, 389-392.

Tagliabue, A., Arrigo, K.R., 2003. Anomalously low zooplankton abundance in the Ross Sea: An alternative explanation. Limnol Oceanogr 48, 686-699.

Tagliabue, A., Arrigo, K.R., 2005. Iron in the Ross Sea: 1. Impact on CO2 fluxes via variation in phytoplankton functional group and non-Redfield stoichiometry. J Geophys Res 110, C03009.

Tagliabue, A., Bopp, L., Aumont, O., 2008. Ocean biogeochemistry exhibits contrasting responses to a large scale reduction in dust deposition. Biogeosciences 5, 11-24.

Welschmeyer, N.A., 1994. Fluorometric analysis of chlorophyll-*a* in the presence of chlorophyll-b and pheopigments. Limnol Oceanogr 39, 1985-1992.

691 Wu, H., Cockshutt, A.M., McCarthy, A., Campbell, D.A., 2011. Distinctive
692 Photosystem II Photoinactivation and Protein Dynamics in Marine Diatoms. Plant
693 Physiology 156, 2184-2195.
694

695 **Tables and Fig. Legends**

696

697 **Table 1** Locations for long-term experiments conducted during NBP12-01 along with values
698 of initial F_v/F_m, $\Delta(F_v/F_m)$ (Equation 1), net growth rates estimated from chlorophyll
699 accumulation (Supplementary Information, Equation S1) and nitrate drawdown
700 (Supplementary Information, Equation S2) over 168 h. Shown are averages ± standard errors
701 (n = 3 or 5), * indicate significant differences (Two-way ANOVA, $p<0.05$) from control.

702

703 **Fig. 1 Composite map of Southern Ocean MODIS chlorophyll *a* for December 2011 –**
704 **February 2012. Inset:** Long-term (blue dots) and short-term (red dots) experimental locations
705 conducted on cruise NBP12-01 in the Ross Sea with 250 m bathymetric contours. Surface *in*
706 *situ* samples were also collected at these locations and at those marked CTD-station (black
707 dots).

708

709 **Fig. 2** Surface chlorophyll concentrations (μg L^{-1}) from CTD stations **(a)**. Surface DIN
710 concentrations (μM) **(b)**. Surface F_v/F_m **(c)**. Surface DFe concentrations (nM) **(d)**. Chlorophyll,
711 DIN and F_v/F_m from samples collected at 1-5 m depth, DFe from samples collected at ~10 m
712 depth.

713

714 **Fig. 3** Matrix of Pearson's linear correlation coefficients between the variables measured in the
715 surface waters of the Ross Sea, including: sea surface temperature (SST), Nitrate (DIN),
716 Phosphate (PO_4^{3-}), Silicate (Si), community structure (% Diatoms), chlorophyll concentration,
717 F_v/F_m, σ_{PSII}, F_m:PsbA, Chl:PsbA, and dissolved iron concentrations (DFe). The strength of the
718 linear association between each pair of variables is indicated by the colour of the square, with
719 the negative and positive correlations denoted by '-' and '+' within all squares where
720 significant ($p<0.01$).

721

722 **Fig. 4** Spatial distribution of $\Delta(F_v/F_m)$ calculated from Fe addition incubation experiments **(a)**.
723 $\Delta(F_v/F_m)$ calculated from long-term Fe-addition incubation experiments in the Ross Sea, both
724 from (1) near the Ross Ice Shelf, (2) over the Ross Bank and (3) within an anti-cyclonic eddy
725 **(b)**. The change in chlorophyll normalized maximum fluorescence, (ΔF_m Chl^{-1}) from the three
726 long-term Fe addition incubation experiments **(c)**. The change in chlorophyll normalized
727 variable fluorescence $\Delta(F_v$ $Chl^{-1})$ from the three long-term Fe addition incubation experiments

728 **(d)**. Shown are averages with ± standard errors (n = 4 or 5). * represent statistically significant
729 differences (*t-test*, p<0.05).
730
731 **Fig. 5** Relationship of DIN (μM) and photosynthetic efficiency (F_v/F_m) throughout the Ross
732 Sea as a function of a) chlorophyll concentrations (μg L^{-1}), b) phytoplankton composition (%),
733 and c) the relative degree of Fe stress $\Delta(F_v/F_m)$ **(c)**. Grey dots represent stations where DIN and
734 F_v/F_m were measured but no corresponding additional variables were measured.
735
736 **Fig. 6** Relationship of DIN (μM) and photosynthetic efficiency (F_v/F_m) throughout the Ross
737 Sea as a function of a) functional cross-section of photosystem II (σ_{PSII}) (nm^{-2}), b) the ratio of
738 chlorophyll to PsbA (a core subunit of PSII) (mmol mol^{-1}), c) the ratio of the maximum
739 fluorescence yield to chlorophyll (F_m:Chl), and d) the ratio of the maximum fluorescence yield
740 to PsbA (F_m:PsbA). Grey dots represent stations where DIN and F_v/F_m were measured but no
741 corresponding additional variables were measured.
742

743 Table 1

744

Experiment	**1**	**2**	**3**
Lat (°S)	75.72	76.72	77.55
Long (°W)	183.40	179.08	175.97
$F_v/F_{m\ Initial}$	0.26 ±0.01	0.29 ±0.00	0.21 ±0.00
$\Delta (F_v/F_m)$, 24 h	0.04 ±0.01	0.00 ±0.00	0.01 ±0.00
$\mu^{Chl}_{Control}$ (d^{-1}), 0 -168 h	0.11 ±0.02	0.25 ±0.01	0.13 ±0.01
μ^{Chl}_{Fe} (d^{-1}), 0 -168 h	0.17* ±0.02	0.29* ±0.00	0.19* ±0.01
ΔNO_3^- Control (μ M d^{-1}), 0 – 168 h	1.61 ±0.33	1.50 ±0.04	2.43 ±0.08
ΔNO_3^- Fe (μ M d^{-1}), 0 – 168 h	2.53* ±0.13	1.57 ±0.05	2.93* ±0.07

745

746 Fig. 1

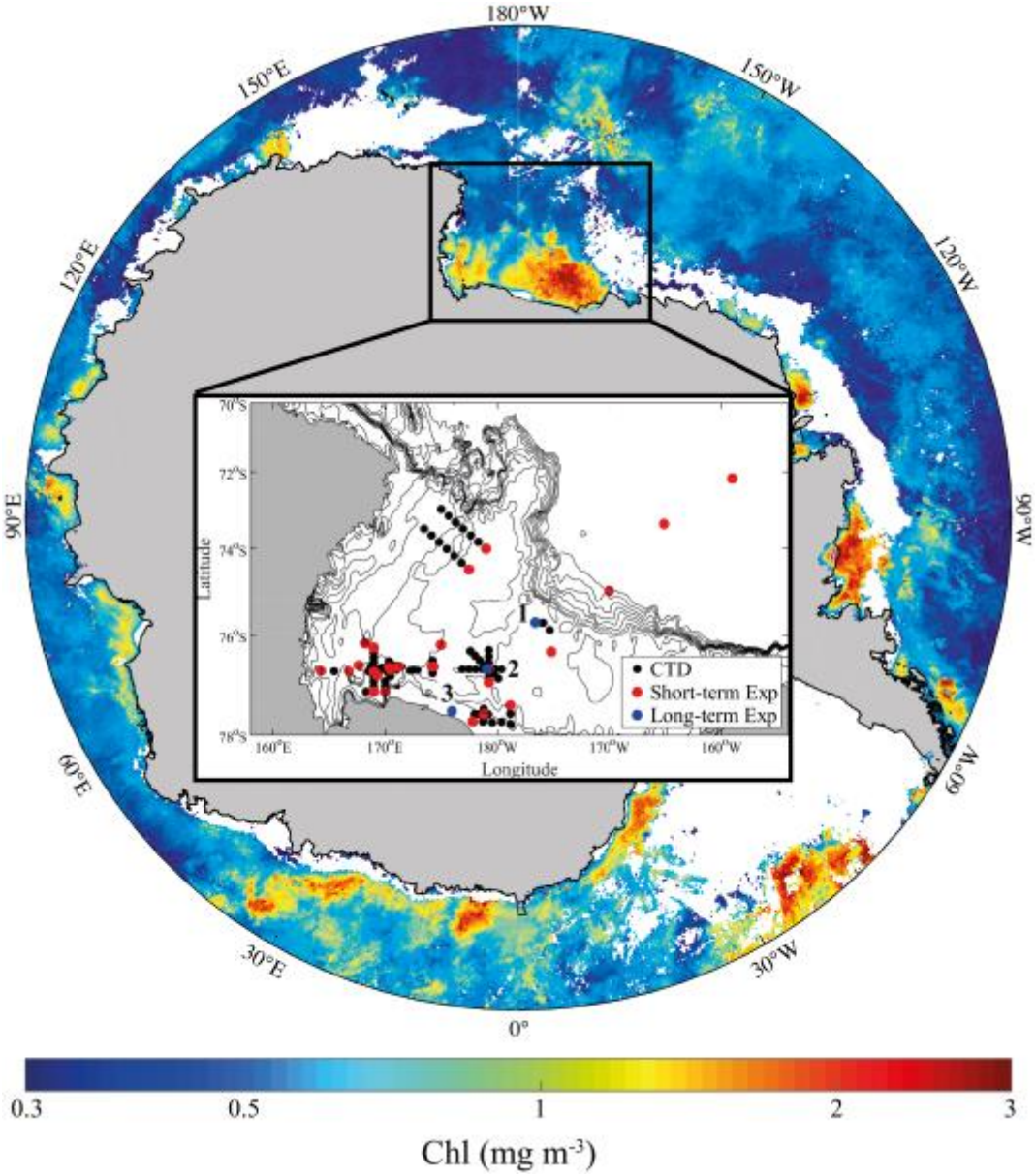

747

748

749 Fig. 2

750

751

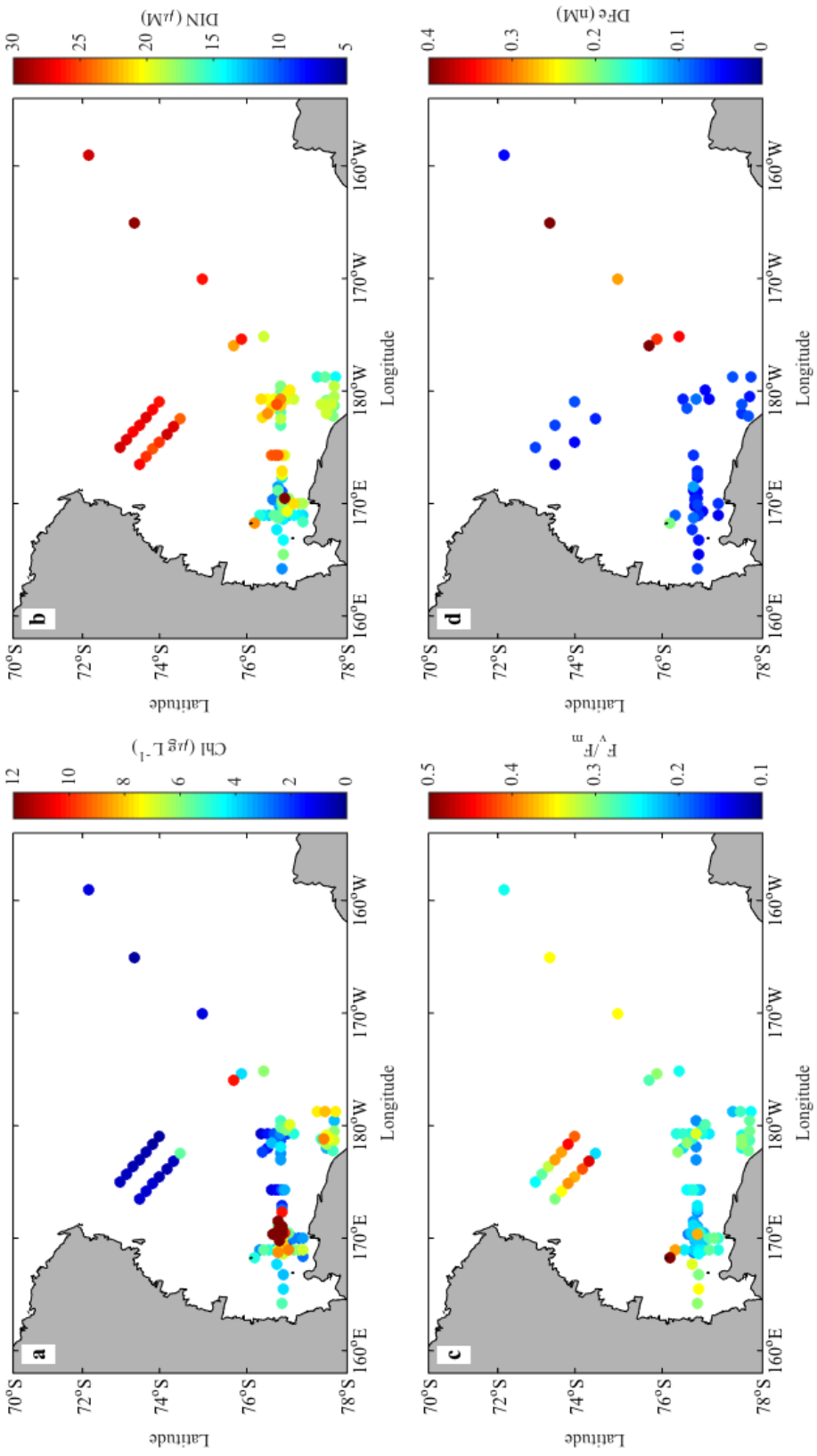

752 Fig. 3

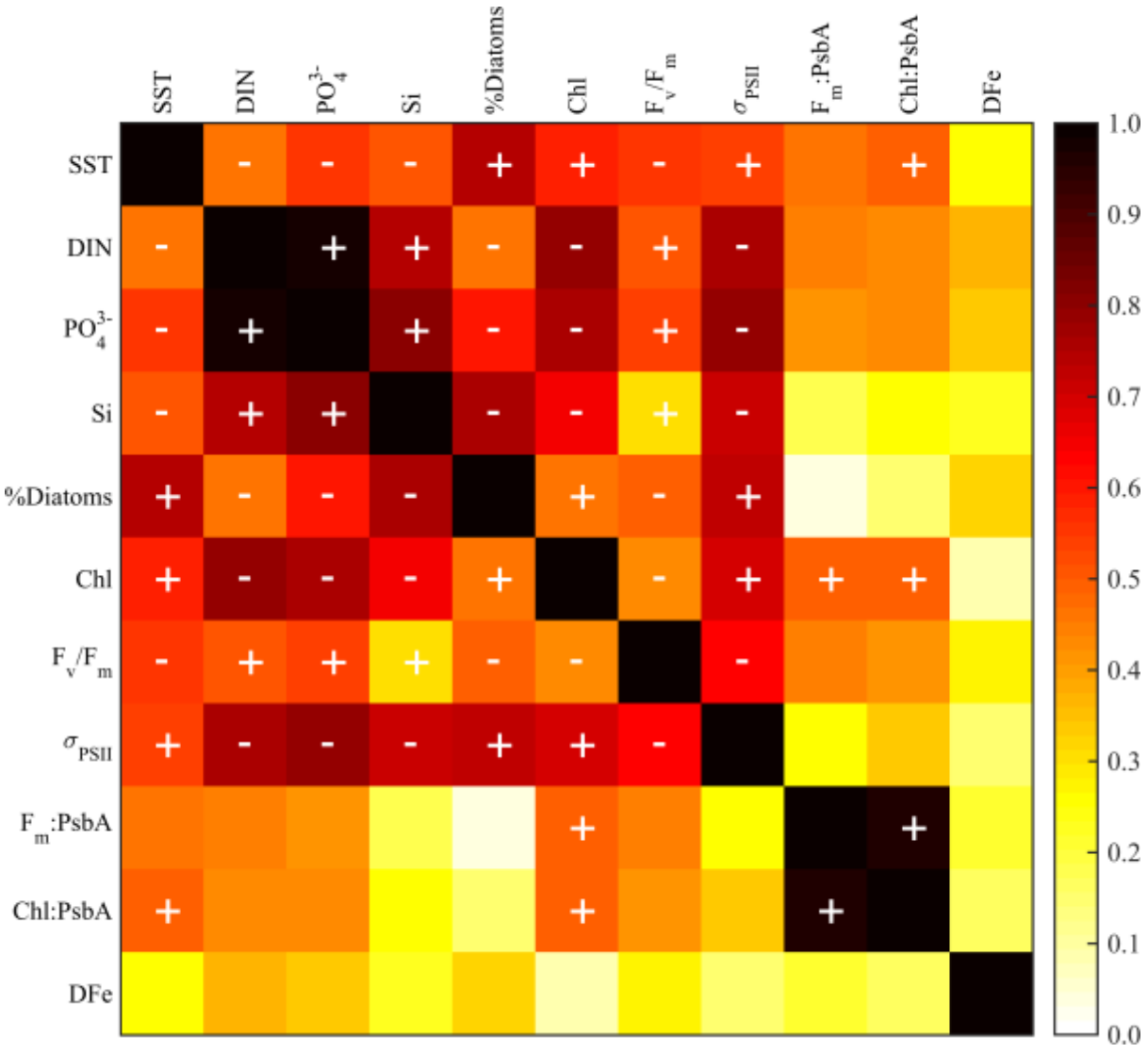

753

754

755 Fig. 4

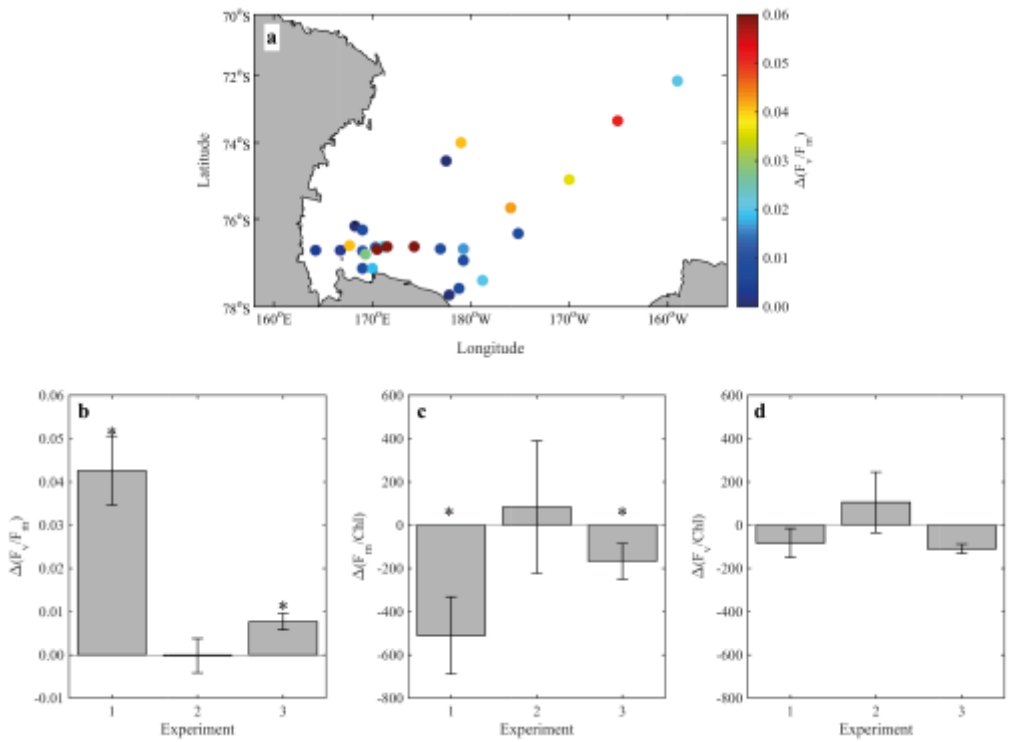

756

757

758 Fig. 5

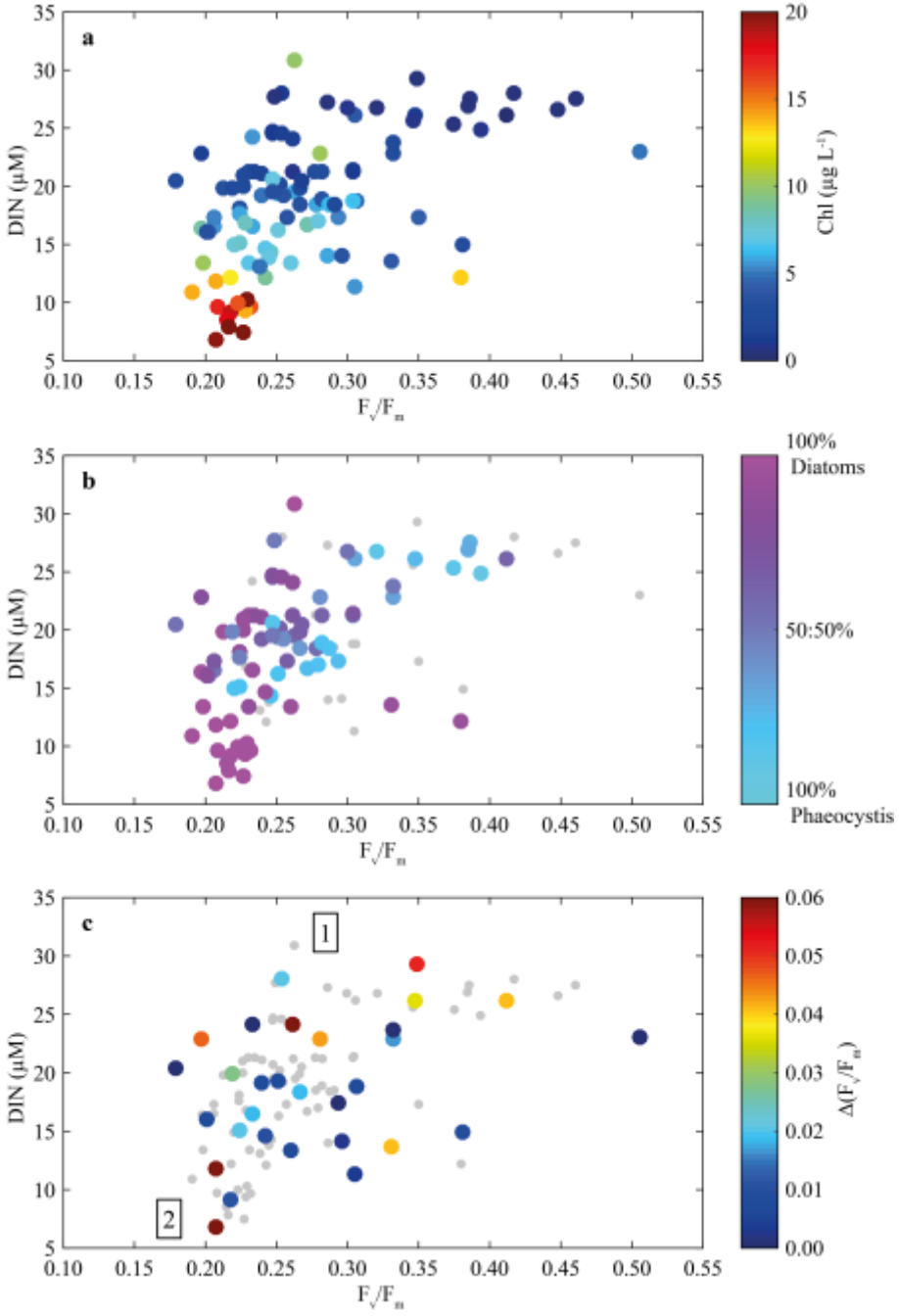

759

760

761 Fig. 6

762

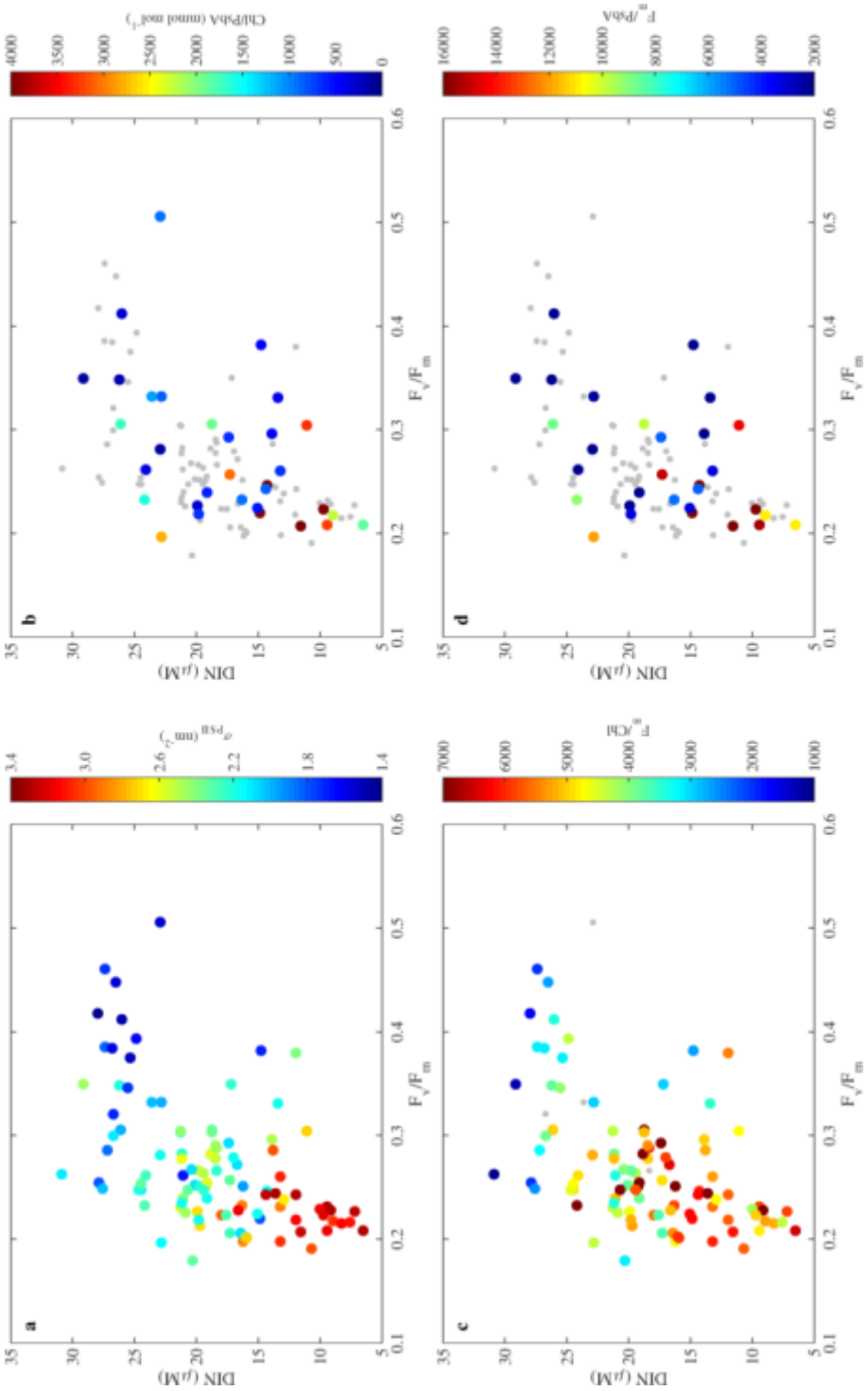

Supplementary Information

Equation S1 Equation for the calculation of chlorophyll-derived net growth rates.

$$\mu^{Chl} = \frac{\ln\left(Chl_{t=168}/Chl_{t=0}\right)}{t}$$

where t = time in hours

Equation S2 Equation for the calculation of nitrate removal.

$$\Delta NO_3^- = \frac{\left[NO_3^-{}_{t=168}\right] - \left[NO_3^-{}_{t=0}\right]}{t}$$

Figure S1 Linear regression correlation matrices of surface variables measured in the Ross Sea. Black dots represent the data points, with black line indicating the linear regression fit with the grey shaded areas the 95% confidence interval limits.